EXPLORING THE EPILEPTIC NETWORK WITH PARALLEL ICA OF INTERICTAL EEG-FMRI

B. Hunyadi[*†], *M. De Vos*[‡], *W. Van Paesschen*[§¶], *S. Van Huffel*[*†]

[*] STADIUS Center for Dynamical Systems, Signal Processing and Data Analytics,
Department of Electrical Engineering (ESAT), KU Leuven, Belgium
[†] iMinds Medical IT, Belgium
[‡] Institute of Biomedical Engineering, Department of Engineering, Oxford University, Oxford, UK
[§] Laboratory for Epilepsy Research, UZ Leuven and KU Leuven, Leuven, Belgium
[¶] Medical Imaging Research Center, UZ Leuven and KU Leuven, Leuven, Belgium

ABSTRACT

The ultimate goal of the EEG-fMRI analysis in refractory focal epilepsy is the precise localization of the epileptogenic zone (EZ) to facilitate successful surgery. Many studies have shown that simultaneous GLM-based EEG-correlated fMRI analysis can identify fMRI voxels which covary with the timing of interictal spikes assessed on EEG. However, this type of analysis often does not reveal a single focus but an extensive epileptic network. In this paper we investigate whether parallel independent component analysis (ICA), a data-driven, symmetric integration approach can disentangle this network. We assume that ICA of EEG and ICA of fMRI will reveal different temporal and spatial aspects of this network, respectively. We hypothesize that by matching these different epilepsy-related EEG and fMRI components, we can get a deeper insight in the neural processes this extensive network represents. We tested parallel ICA on 12 refractory epilepsy patients who underwent full presurgical evaluation and showed concordant data (excluding EEG-fMRI) pointing to a single epileptic focus. Our results show that parallel ICA has an added value, as it can help the interpretation of the GLM results and pinpoint the EZ. Furthermore, it might help to understand how the various aspects of epileptic activity are reflected in EEG and fMRI.

Index Terms— ICA, parallel ICA, EEG, fMRI, epilepsy

1. INTRODUCTION

Refractory epilepsy patients continue to suffer from seizures despite of anti-epileptic medication. In focal epilepsy, where the seizures are generated in a certain confined brain region, surgical resection can offer a remedy. The resection or disconnection of the epileptogenic zone (EZ), by definition, is necessary and sufficient for seizure freedom. Simultaneous EEG-fMRI analysis was shown to be useful in the presurgical work-up of epilepsy [1]. Within the general linear model (GLM) framework, a regressor is defined based on the timing of the interictal spikes observed in the EEG. This regressor is then used to find voxels showing similar blood oxygen level dependent (BOLD) fMRI signal fluctuations. The GLM results often show widespread activations in the brain. Some studies claim that such widespread activations reflect multifocality, i.e. distributed epileptogenic tissue, while others argue that it reflects interregional interactions between the EZ and other remote sites, in line with the hypothesis that epilepsy is a network disorder [2].

Technically speaking, the mismatch between the temporal dynamics of EEG and fMRI limits the capabilities of GLM analysis. As the BOLD signal in response to a transient neural event peaks after several seconds, fMRI cannot differentiate the nuances of all underlying neural processes which are reflected in the millisecond resolution EEG. Therefore, the fine temporal details of EEG are lost in such a model-based approach. Alternatively, many studies applied independent component analysis (ICA) either to decompose EEG and define a more specific regressor for GLM [3,4] or to decompose fMRI and select the epileptic component based on spike timing information [5] or using machine learning in the absence of spikes [6]. Such data-driven approaches efficiently exploit the entire underlying data structure. As a result, activation maps more specific to the EZ may be obtained. Here we propose a symmetric approach based on parallel ICA: we analyze both EEG and fMRI in a data-driven way to reveal different spatial and temporal processes in both modalities and then match the resulting components. This way we find multiple pairs of corresponding EEG-fMRI components. This will not only allow to pinpoint the EZ by disentangling onset from propagation, but also to understand how various underlying epileptic processes are reflected in one modality and the other.

978-0-9928626-3-3/15/$31.00 ©2015 IEEE

2. METHODS

2.1. Data acquisition and preprocessing

Simultaneously recorded EEG and fMRI data were acquired from 12 refractory focal epilepsy patients. All patients underwent full presurgical evaluation for epilepsy surgery and had concordant data. 8 patients were operated on with good surgical outcome (ILAE score 1-3), while surgery was not performend in the other 4 cases as the EZ was in eloquent cortex. EEG-fMRI data were recorded prior to surgery, but the results were not taken into account within the presurgical evaluation. The EZ was determined based on the post-operative MRI, if available (5 cases), or as the SISCOM hyperperfusion area within the hypothetical resection zone, otherwise. The EZ of each patient is reported in Table 1 on the level of lobes for simplicity, even if the EZ was more concise.

Functional images were acquired using a whole-brain single-shot T2* Gradient-Echo Echo Planar Imaging sequence in one of two 3 Tesla MR-scanners (Achieva TX with a 32-channel head coil and Intera Achieva with an 8-channel head coil, Philips Medical Systems, Best, The Netherlands); echo time = 33 ms, repetition time 2.2-2.5 s, voxel size: 2.6 x 3 x 2.6 mm^3. All fMRI images were realigned, slice-time corrected, normalized to MNI space using the coregistered high-resolution structural scan (resampled voxel size 2 x 2 x 2 mm^3) and spatially smoothed with an isotropic Gaussian kernel of 6 mm full width at half maximum using statistical parametric mapping (SPM8, Wellcome Department of Imaging Neuroscience, University College London, UK; available at `http://www.fil.ion.ucl.ac.uk/spm/`).

EEG data were recorded with a 24-channel or 32-channel MR-compatible EEG system while the patients rested with closed eyes. After offline bandpass filtering between 1-50Hz gradient artifacts and pulse artifacts were removed using the Bergen plug-in (Bergen fMRI Group,Bergen,Norway) and with Brain Vision Analyzer software (BrainProducts, Munich, Germany), respectively. Subsequently, spikes were marked by a neurologist.

2.2. GLM-based analysis

EEG-correlated fMRI analysis was performed within the GLM framework. The timing of the most frequent spike type convolved with the canonical hemodynamic response function (HRF, provided in SPM8) was used as a regressor of interest. The six rigid-body motion correction parameters, the fMRI signal averaged over the lateral ventricles, and the signal averaged over a region centered in the white matter were included as confounding covariates. The activation maps were thresholded at $z > 3.5$ and only clusters containing at least 350 voxels were retained. These settings were shown to be the most sensitive ones to the EZ at 100% specificity [2].

2.3. Parallel ICA

EEG provides a volume conducted and spatially undersampled representation of a mixture of various independent neural processes. Similarly, these processes exhibit a spatially mixed and temporally degraded BOLD signal on fMRI. In order to disentangle the multiple sources of variability in each modality, ICA of EEG and fMRI is performed separately and then the sources are matched based on the similarity of their temporal fluctuations. This approach, called parallel ICA, has been applied in [7] to decompose multisubject EEG-fMRI data. Here, we apply it on a patient-by-patient basis. Furthermore, we adapted the matching procedure (see 2.3.3) to take into account the entire time span of the recordings instead of looking at only trial-by-trial fluctuations. The different steps of parallel ICA are explained in the following sections.

2.3.1. Temporal ICA of EEG

We assume that the multichannel EEG $X_{EEG} \in \mathbb{R}^{C \times T_{EEG}}$ observed over C channels and T_{EEG} number of time samples, is a linear mixture of N underlying independent source signals. Then, X_{EEG} can be written as follows:

$$X_{EEG} = A_{EEG} S_{EEG}. \quad (1)$$

The rows of the source matrix $S_{EEG} \in \mathbb{R}^{N \times T_{EEG}}$ contain the underlying sources, while the mixing matrix $A_{EEG} \in \mathbb{R}^{C \times N}$ describes the mixing system. In other words, each column of the mixing matrix describe the relative strength of a given source on each channel, i.e. the scalp topography of the source. The number of underlying components N was estimated as the median of the values obtained by the Minimum Description Length, Akaike and Bayesian Information Criteria. The independent components (ICs) were estimated using the Infomax algorithm [8].

2.3.2. Spatial ICA of fMRI

We assume that the BOLD signal fluctuations $X_{fMRI} \in \mathbb{R}^{T_{fMRI} \times V}$ observed over V voxels and T_{fMRI} time samples are generated by M independent sources which are organized independently in space:

$$X_{fMRI} = A_{fMRI} S_{fMRI}. \quad (2)$$

Here the rows of the source matrix S_{fMRI} represent the spatial maps, i.e. the organization of each source in the voxel space. The columns of the mixing matrix A_{fmri} describe the time course of each source, i.e. how the strength of their activity fluctuates over time. The decomposition was performed using The Probabilistic ICA algorithm provided in MELODIC, FSL toolbox (`http://fsl.fmrib.ox.ac.uk/fsl/fslwiki/`), including the automatic estimation of the number of ICs using a Bayesian framework.

Patient	EZ	GLM map	# EEG eICs	# fMRI eICs	# matches	Conclusive
1	LT	widespread	2 (9)	5 (97)	1	**Yes** Single fMRI-eIC overlaps with the EZ.
2	LT	LT activation	4 (8)	2 (103)	1	**Yes** Only fMRI-eIC67 has matched EEG-eICs. This map overlaps better with the EZ than the other fMRI-eIC.
3	RT	no activation	5 (8)	3 (68)	3	**No** Mutliple matching EEG-fMRI components, the network cannot be disentangled.
4	LP	widespread	5 (8)	1 (132)	1	**No** Single fMRI-eIC has occipital activation, not overlapping with the EZ.
5	RT	widespread	2 (4)	2 (86)	0	**No** No EEG-fMRI-eIC matches.
6	RTP	widespread	2 (5)	1 (60)	1	**No** Single fMRI-eICs overlaps with the GLM activation map at multiple clusters (including the EZ).
7	LT	LT activation	3 (8)	2 (48)	0	**No** No EEG-fMRI-eIC matches.
8	RF	widespread	5 (10)	1 (78)	1	**Yes** Single fMRI-eIC overlaps with the EZ.
9	LT	widespread	3 (7)	5 (50)	5	**Yes** The EEG-eIC which correlates best with the template topography matches fMRI-eIC3 which overlaps with the GLM activation maps at the EZ. fMRI-eICs with occipital activation are correlated to multiple EEG-eICs which reflect propagated activity (different topography or slow wave morphology with a late peak.)
10	LTO	no activation	3 (5)	5 (85)	3	**Yes** EEG-eIC most similar to the template topography matches with an fMRI-eIC reflecting the EZ. Other EEG-eICs which reflect propagated activity (slow wave morphology with a late peak or related to the secondary spike type) match fMRI-eICs reflecting other parts of the epileptic network remote from the EZ.
11	RT	no activation	5 (9)	1 (90)	1	**Yes** The single fMRI-eIC overlaps with the EZ.
12	LT	LT activation	6 (8)	2 (99)	1	**Yes** Only fMRI-eIC78 has matched EEG-eICs. This map overlaps with the EZ.

Table 1. True epileptogenic zone (EZ), GLM and Parallel ICA results of the patients. Next to the number of eICs the total number of ICs are indicated in brackets. Abbreviations: R: right L:left T: temporal F: frontal P: parietal O: occipital

2.3.3. EEG-fMRI component matching

First, the subset of epilepsy-related independent components (eICs) were selected as follows.

For EEG, a spike template was obtained by temporal averaging of the spikes marked by the neurologists. Averaging was time-locked to the largest negative peak of the spike. Then, the scalp topography at 50% of the rising phase of the average spike was taken [9], along with the time course of the spike on the channel where the negative deflection was the largest. In case multiple spike types were present, a template for all of them were created. Similarly, an average IC spike was obtained by averaging the IC time course time-locked to the marked spikes. The topography of the ICs were obtained from the corresponding column of the mixing matrix. Then, ICs which significantly correlated ($p < 0.05$, Pearson's correlation) both in time course and in spatial distribution with either of the spike templates were labeled as epilepsy-related (EEG-eICs).

For fMRI, the spatial maps of the ICs were compared to the GLM activation maps, while the IC time courses were compared to the regressor of interest. ICs which showed significant correlation to the regressor ($p < 0.05$) and to the GLM activation maps ($p < 0.05$ and $r > 0.1$) were labeled as epilepsy related (fMRI-eICs). In the latter case constraining the correlation coefficient was necessary, because significance at $p < 0.05$ was easily reached due to the large number of voxels ($n > 5 \cdot 10^5$). In cases where no significant GLM activations were present, the unthresholded GLM maps were used. Afterwards, the fMRI spatial maps were normalized to z-scores by subtracting the mean voxel value and dividing with the standard deviation and were thresholded at $|z| \leq 5$. The selected fMRI ICs were visually inspected and those containing a majority of suprathreshold voxels in the ventricles or in the white matter were rejected.

Subsequently, the epilepsy related EEG and fMRI components were matched based on their time courses. In order to account for the difference in their temporal dynamics the time courses of the EEG ICs were convolved with the canonical hemodynamic response function and the time courses of the fMRI time courses were upsampled to match the sampling rate of the EEG. Then, Pearson's correlation coefficient $r_P$was computed for all possible EEG-fMRI IC

pairs. A match was established if $r_P > 0.1$.

3. RESULTS

Results obtained using GLM-based analysis and parallel ICA are summarized in Table 1. The GLM activation map showed a single activation cluster overlapping with the EZ in 3 out of 12 cases. In 6 cases it showed activation both in the EZ and in one or more remote areas. Finally, in 3 cases no significant activation was present.

Multiple epileptic EEG-eICs were found in all cases. A single fMRI-eIC was found in 4 patients and multiple fMRI-eICs were found in 8 patients. Parallel ICA found no matching EEG-fMRI IC pairs in patients 5 and 7. A matching EEG-eIC was found for a single fMRI-eIC in 7 cases. In 6 out of these 7 cases this fMRI-eIC overlapped with the EZ, however, in 1 case it also overlapped with other clusters in the GLM activation map. In 3 further patients parallel ICA found a matching EEG-eIC for at least 2 fMRI-eICs. In 2 of these cases (patients 9 and 10) the EEG-eIC most similar to the spike template in topography matched that particular fMRI-eIC which overlaps with the GLM map in the EZ. Other EEG-eICs which were less similar to the spike template matched an fMRI-eIC overlapping with the GLM map in a region remote to the EZ. In the last case (patient 3) multiple matching EEG-fMRI IC pairs were found, therefore, the epileptic network could not be disentangled.

In summary, while GLM revealed focal activations in only 3 cases, parallel ICA could reveal the EZ in 7 cases. Although the results were inconclusive in 5 patients, in 4 of them they were not misleading either.

In order to illustrate our findings on a concrete case, we show the epileptic network of patient 10, as revealed by parallel ICA in Figure 1. This patient had 3 epileptic EEG and 5 epileptic fMRI components. The second epileptic EEG component (EEG-IC2) is most similar to the spike template both in its time course and its topography. EEG-IC1 resembles the secondary spike type of this patient over the temporal area, while EEG-IC3 shows a deflection a few milliseconds later than the mean spike peak. Therefore, EEG-IC2 can be associated with onset type activity, while EEG-IC1 and EEG-IC3 can be associated with propagated activity. Each of these 3 ICs have a matching fMRI component. EEG-IC2 matched to fMRI-IC62 and fMRI-IC21. While fMRI-IC62 was matched exclusively to EEG-IC2, fMRI-IC21 matched with both propagated EEG ICs as well. Finally, EEG-IC1 matched fMRI-IC20. From this one can deduce that fMRI-IC62 represents the onset region of the epileptic activity, while the fMRI-IC20 and fMRI-IC21 are involved at a later phase of epileptiform activity. Notably, the spatial map of fMRI-IC62 coincides best with the zone of surgical resection which rendered the patient seizure free.

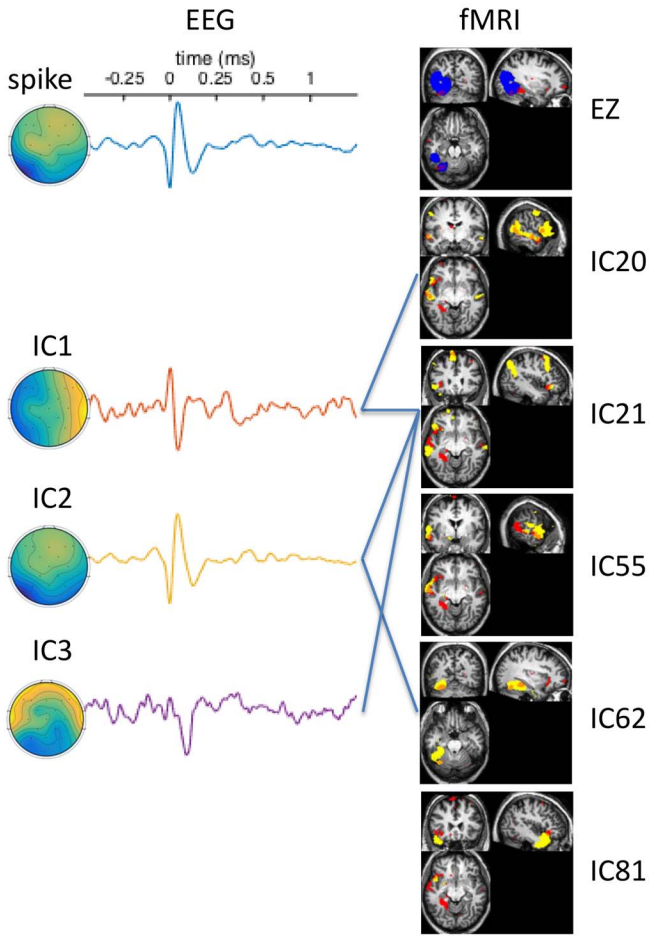

Fig. 1. The epileptic network of patient 10. The spike template, the EZ (blue) and the GLM activation map (red) are shown on the top. Note that none of the GLM clusters exceed 350 voxels threshold, we nevertheless show them for comparison with the IC maps. The epilepsy related EEG and fMRI components (yellow) are shown on the left and on the right, respectively. The matching EEG and fMRI components are connected with blue lines.

4. DISCUSSION

Our results showed that parallel ICA can help the interpretation of the extensive GLM activation maps in the following way. In case a single EEG-fMRI-eIC pair is selected, the spatial map of the fMRI-IC correctly indicated the EZ. In cases where multiple EEG-fMRI-eIC pairs were found, the fMRI-eICs can be interpreted based on their EEG-eIC pairs. Those fMRI-eICs which matched exclusively the EEG-eICs most similar to the spike template overlapped with the GLM map at the EZ (type 1 EEG-fMRI eICs). Other EEG-eICs which were less similar to the spike template matched an fMRI-eIC overlapping with the GLM map in a region remote to the EZ (type 2 EEG-fMRI eICs). The significance of this finding is

twofold. First, it shows that the parallel ICA approach can help in the objective identification of the EZ and facilitate successful surgical resection and seizure freedom. Moreover, parallel ICA may shed the light on different mechanisms underlying the epileptic network activity. Type 1 EEG-fMRI eICs can be interpreted as electrographical and BOLD correlates of primary, onset-type epileptic activity. The spatial maps of type 2 EEG-fMRI-eICs were often similar to well-known resting state networks (RSNs). Notably, many recent studies have shown that RSNs are impaired in epilepsy patients. The characteristics of the type 2 EEG components were somewhat heterogeneous. In patient 10 it was similar to the secondary spike type of the patient, while in others they reflected a slow-wave like morphology, i.e. less sharp than the spike template and with a later occurring peak. Interestingly, such slow waves in epilepsy are associated with inhibitory mechanisms or propagated activity. The existence of type 2 EEG-fMRI-eICs suggest that slow waves might be the electrographical correlates of the same neuronal processes which cause an altered RSN activity in epilepsy patients.

The proposed parallel ICA-based approach has some limitations. The matching procedure was restricted to EEG-eICs and fMRI-eICs selected based on the spike templates in EEG and the GLM results. In patient 5, 7, 10 and 12 more than one spike types were present. In patients 5 and 7 the parallel ICA results were not satisfactory, suggesting that the epileptic activity is more complex and may require more involved analysis in these cases. Moreover, there might be epilepsy related potential fluctuations which are not time-locked to the spike occurrences, or might be better characterized in frequency than in time domain [4]. Similarly, there might be impaired networks in areas different from the GLM activation clusters. Such aspects of epileptic activity are hidden from our methodology. Furthermore, GLM activation maps were obtained using the canonical HRF. Including its derivatives or other basis functions, such as FIR models, may improve the results. Finally, parallel ICA decomposes EEG and fMRI independently from each other. Other data fusion approaches, like jointICA [10, 11] or joint matrix/tensor factorizations [12, 13] could decompose EEG and fMRI simultaneously, facilitating mutual information flow between the modalities within the decomposition. Although this implies the very strong assumption of both modalities sharing the same linear mixing system, they might provide results complementary to parallel ICA.

5. ACKNOWLEDGMENTS

Research Council KUL: CoE PFV/10/002 (OPTEC), PhD/Postdoc grants, Flemish Government: FWO: projects: G.0427.10N (Integrated EEG-fMRI), G.0108.11 (Compressed Sensing) G.0869.12N (Tumor imaging) G.0A5513N (Deep brain stimulation), PhD/Postdoc grants; IWT: projects: TBM 080658-MRI (EEG-fMRI), TBM 110697-NeoGuard; PhD/Postdoc grants iMinds Medical Information Technologies SBO 2015, ICON: NXT_Sleep; Belgian Federal Science Policy Office: IUAP P7/19/ (DYSCO, "'Dynamical systems, control and optimization"', 2012-2017); Belgian Foreign Affairs-Development Cooperation: VLIR UOS programs; EU: The research leading to these results has received funding from the European Research Council under the European Union's Seventh Framework Programme (FP7/2007-2013) / ERC Advanced Grant: BIOTENSORS (n^o 339804).This paper reflects only the authors' views and the Union is not liable for any use that may be made of the contained information; other EU funding: RECAP 209G within INTERREG IVB NWE programme, EU MC ITN TRANSACT 2012 (n^o 316679), ERASMUS EQR: Community service engineer (n^o 539642-LLP-1-2013)

REFERENCES

[1] M. Zijlmans, G. Huiskamp, M. Hersevoort, J.-H. Seppenwoolde, A. C. van Huffelen, and F. S. S. Leijten, "EEG–fMRI in the preoperative work–up for epilepsy surgery," *Brain*, vol. 130, no. 9, pp. 2343–2353, 2007.

[2] S. Tousseyn, P. Dupont, K. Goffin, S. Sunaert, and W. Van Paesschen, "Sensitivity and specificity of interictal EEG-fMRI for detecting the ictal onset zone at different statistical thresholds," *Front Neurol*, vol. 5, no. 1–11, pp. 279–311, 2014.

[3] J. P. Marques, J. Rebola, P. Figueiredo, A. Pinto, F. Sales, and M. Castelo-Branco, "ICA decomposition of EEG signal for fMRI processing in epilepsy," *Hum brain mapp*, vol. 30, no. 9, pp. 2986–2996, 2009.

[4] M. Leite, A. Leal, and P. Figueiredo, "Transfer function between EEG and BOLD signals of epileptic activity," *Front Neurol*, vol. 4, no. 1, pp. –, 2013.

[5] P. LeVan, L. Tyvaert, and J. Gotman, "Modulation by EEG features of BOLD responses to interictal epileptiform discharges," *Neuroimage*, vol. 50, no. 1, pp. 15–26, 2010.

[6] B. Hunyadi, S. Tousseyn, P. Dupont, S. Van Huffel,M. De Vos and W. Van Paesschen, "A prospective fMRI-based technique for localising the epileptogenic zone in presurgical evaluation of epilepsy," in *Neuroimage*, vol. 113, pp. 329–339., Jun. 2015

[7] T. Eichele, V. D. Calhoun, M. Moosmann, K. Specht, M. L. A Jongsma, R. Q. Quiroga, H. Nordby, and K. Hugdahl, "Unmixing concurrent eeg-fmri with parallel independent component analysis," *Int J of Psychophysiol*, vol. 67, no. 3, pp. 222–234, 2008.

[8] A. J. Bell and T. J. Sejnowski, "An information–maximization approach to blind separation and blind deconvolution," *Neural Comput*, vol. 7, no. 6, pp. 1129–1159, Nov. 1995.

[9] M. Seeck, F. Lazeyras, C. Michel, O. Blanke, C. Gericke, J. Ives, J. Delavelle, X. Golay, C. Haenggeli, N. De Tribolet and T. Landis, "Non-invasive epileptic focus localization using EEG-triggered functional MRI and electromagnetic tomography," *Electroencephalography and clinical Neurophysiology*, vol. 106, no. 6, pp. 508-512, 1998.

[10] V. D. Calhoun, T. Adali, G. D. Pearlson, and K. A. Kiehl, "Neuronal chronometry of target detection: Fusion of hemodynamic and event–related potential data," *NeuroImage*, vol. 30, no. 2, pp. 544 – 553, 2006.

[11] B. Mijović, K. Vanderperren, N. Novitskiy, B. Vanrumste, P. Stiers, B. Van den Bergh, L. Lagae, S. Sunaert, J. Wagemans, S. Van Huffel, and M. De Vos, "The "why" and "how" of jointICA: Results from a visual detection task," *NeuroImage*, vol. 60, no. 2, pp. 1171 – 1185, 2012.

[12] E. Acar, T. G. Kolda, and D. M. Dunlavy, "All-at-once optimization for coupled matrix and tensor factorizations," *arXiv preprint arXiv:1105.3422*, 2011.

[13] L. Sorber, M. Van Barel, and L. De Lathauwer, "Structured data fusion," *IEEE J Sel Top Signa*, p. accepted, 2015.